



Contents lists available at ScienceDirect

Chinese Herbal Medicines

journal homepage: www.elsevier.com/locate/chmed

Original Article

Neuroprotective effects of Longxue Tongluo Capsule on ischemic stroke rats revealed by LC-MS/MS-based metabolomics approach

Jing Sun^{a,b,1}, Xianyang Chen^{c,1}, Yongru Wang^b, Yuelin Song^a, Bo Pan^a, Bei Fan^b, Fengzhong Wang^b, Xiaonan Chen^a, Pengfei Tu^a, Jiarui Han^c, Huixia Huo^{a,*}, Jun Li^{a,*}^a Modern Research Center for Traditional Chinese Medicine, School of Chinese Materia Medica, Beijing University of Chinese Medicine, Beijing 100029, China^b Key Laboratory of Agro-products Quality and Safety Control in Storage and Transport Process, Laboratory of Agro-products Quality Safety Risk Assessment, Ministry of Agriculture, Institute of Food Science and Technology, Chinese Academy of Agricultural Sciences, Beijing 100193, China^c Baofeng Key Laboratory of Genetics and Metabolism, Zhongguancun Biological and Medical Big Data Center, Beijing 101300, China

ARTICLE INFO

Article history:

Received 2 June 2022

Revised 12 August 2022

Accepted 9 December 2022

Available online 25 May 2023

Keywords:

ischemic stroke

Longxue Tongluo Capsule

metabolomics

middle cerebral artery occlusion

phenolic compounds

UHPLC-Q Exactive MS

ABSTRACT

Objective: The present study aimed to evaluate the therapeutic effect and explore the underlying mechanisms of Longxue Tongluo Capsule (LTC) on ischemic stroke rats.**Methods:** Twenty-six rats were randomly divided into four groups, including sham group, sham + LTC group, MCAO group, and MCAO + LTC group. Ischemic stroke rats were simulated by middle cerebral artery occlusion (MCAO), and LTC treatment group were orally administrated with 300 mg/kg of LTC once daily for seven consecutive days. LTC therapy was validated in terms of neurobehavioral abnormality evaluation, cerebral infarct area, and histological assessments. The plasma metabolome comparisons amongst different groups were conducted by UHPLC-Q Exactive MS in combination with subsequent multivariate statistical analysis, aiming to finding the molecules in respond to the surgery or LTC treatment.**Results:** Intra-gastric administration of LTC significantly decreased not only the neurobehavioral abnormality scores but also the cerebral infarct area of MCAO rats. The interstitial edema, atrophy, and pyknosis of glial and neuronal cells occurred in the infarcted area, core area, and marginal area of cerebral cortex were improved after LTC treatment. A total of 13 potential biomarkers were observed, and Youden index of 11 biomarkers such as LysoPC, SM, and PE were more than 0.7, which were involved in neuroprotective process. The correlation and pathway analysis showed that LTC was beneficial to ischemic stroke rats via regulating glycerophospholipid and sphingolipid metabolism, together with nicotinate and nicotinamide metabolism. Heatmap and ternary analysis indicated the synergistic effect of carbohydrates and lipids may be induced by flavonoid intake from LTC.**Conclusion:** The present study could provide evidence that metabolomics, as systematic approach, revealed its capacity to evaluate the holistic efficacy of TCM, and investigate the molecular mechanism underlying the clinical treatment of LTC on ischemic stroke.© 2023 Tianjin Press of Chinese Herbal Medicines. Published by ELSEVIER B.V. This is an open access article under the CC BY-NC-ND license (<http://creativecommons.org/licenses/by-nc-nd/4.0/>).

1. Introduction

Stroke is a disease featured by local dysfunction of the brain, which is resulted from the disturbance of blood circulation. Currently, stroke is one of the most fatal diseases all over the world, and in recent years, it exhibits a tendency to be happened between young people. There are two primary types of stroke, such as is-

chemic stroke and hemorrhagic stroke, and in particular, ischemic stroke accounts for about 80% of all stroke cases (Lee et al., 2017).

Longxue Tongluo Capsule (LTC) that is derived from the total phenolic compound cluster of Chinese dragon's blood has been approved as a new agent for the clinical treatment of ischemic stroke by China Food and Drug Administration (CFDA) at June 2013. We have demonstrated that LTC possesses anti-atherosclerotic effect, and could improve erythrocyte function against lipid peroxidation (Zheng et al., 2016a, 2016b). Recently, we have also found that LTC can effectively inhibit oxygen-glucose deprivation/reperfusion (OGD/R) induced apoptosis of PC12 cells through suppressing the cleavage of poly ADP-ribose polymerase, caspase-3, and caspase-

* Corresponding authors.

E-mail addresses: huohuixia1989@163.com (H. Huo), drlj666@163.com (J. Li).¹ These authors contributed equally to this work.

9 (Pang et al., 2021). The effective components and pharmacological activity of LTC have been investigated in depth in our groups for years, and the primary constituents of LTC are various phenolic derivatives, the most representative components of which are 7,4'-dihydroxyflavone, 7,4'-dihydroxy-5-methoxyhomoisoflavone, cinnabarone, loureirin A, loureirin B, and other flavonoids (Pang et al., 2016; Pang et al., 2018; Pang et al., 2021; Qin et al., 2015; Su et al., 2014a, 2014b; Sun et al., 2017; Sun et al., 2018; Sun et al., 2019).

Despite of widely applications in clinic and extensive popular in the market, the underlying therapeutic mechanisms are still largely unknown. Metabolomics, through monitoring perturbations in the concentrations of endogenous low molecular weight metabolites (M.w. < 1000) in cells, tissues or biofluids, is able to provide a holistic view to pharmacology, pathology, toxicology or genetics status, which enabled its wide use in disease diagnosis, toxicity screening, drug safety and efficacy assessments, etc. (Zheng et al., 2016a, 2016b; Irie et al., 2014).

The present study aimed to evaluate the effect of LTC towards middle cerebral artery occlusion (MCAO) rats, as well as to disclose the underlying mechanisms of LTC via comparing the plasma metabolome amongst different groups using an LC-MS/MS-based approach. Through subsequently pathway enrichment, we hope to provide pronounced evidences and guidelines for relevant biomarkers clarification.

2. Materials and methods

2.1. Materials and reagents

LC-MS grade methanol, acetonitrile (ACN), and formic acid (FA) were supplied by Thermo-Fisher (Fair Lawn, NJ, USA). Ultrapure water was prepared in-house by a Milli-Q Integral water purification system (Millipore, Bedford, MA, USA).

LTC (Batch No. LTC-140601) was provided by Jiangsu Kanion Pharmaceutical Co., Ltd. (Lianyungang, China). The specimen is deposited at Modern Research Center for Traditional Chinese Medicine, School of Chinese Materia Medica, Beijing University of Chinese Medicine (Beijing, China).

2.2. Animal experiment

All male Sprague-Dawley (SD) rats (280–300 g) were purchased from Beijing SPF Biotechnology Co., Ltd. (Beijing, China). The animals were acclimated in the laboratory for one week prior to the experiments. The animals were housed in an air-conditioned room at (23 ± 1) °C and relative humidity (60 ± 5)% with a 12 h d/night cycle, and all animals were free access to standard chow and tap water. The rats were fasted for 12 h prior to treatment; However, water was provided *ad libitum*. All animal experiment protocols were approved by the Medical Ethics Committee of Beijing University of Chinese Medicine (4-2017041401-2033). All rats were randomly divided into four groups, such as sham group (*n* = 6), sham + LTC group (*n* = 6), MCAO group (*n* = 6), and MCAO + LTC group (*n* = 8).

2.3. Model preparation and drug administration

MCAO model was constructed by following previous descriptions with minor modifications (Longa et al., 1989). Briefly, a short incision was made on rats that was anesthetized with chloral hydrate (300 mg/kg, *i.p.*), and then, right common carotid artery (CCA), external carotid artery (ECA), and internal carotid artery (ICA) were separated. The proximal central end of right CCA as well as ECA was coagulated, and ICA was temporarily clamped with mi-

crovascular clips. Afterwards, a 30-mm length monofilament with a silicon-coated tip (Jialing Biotech Co., Ltd., Guangzhou, China) was directed distally up toward the internal cerebral artery (ICA) to a distance of (17.5 ± 0.5) mm from CCA to occlude the middle cerebral artery. The monofilament was gently removed to allow reperfusion 2.5 h latter. For the sham rats, the right CCA and ECA were exposed without inserting the filament. After surgery, all rats belonging to the LTC treatment group were orally administrated with 300 mg/kg of LTC once daily for seven consecutive days, and rats from sham and MCAO groups were treated in parallel with an equal volume of 0.5% CMCNa.

2.4. Neurobehavioral abnormality evaluation

According to the protocol described previously (Longa et al., 1989), neurobehavioral dysfunction of rats was assessed on a five-point scale: score 0, normal (no neurobehavioral dysfunction); score 1, slight (failure to extend left forepaw fully); score 2, moderate (circling to the left); score 3, severe (falling to the left); score 4, very serious (no autonomous activity and unconsciousness) (Luo et al., 2016).

2.5. Cerebral infarct area measurement

After the cerebellum of the rats was removed, the fresh rat brains were frozen immediately at –20 °C for 30 min. Then, six coronal sections of 2 mm thickness were stained with 1% 2,3,5-triphenyltetrazoliumchloride (TTC) solution in PBS and underwent lucifugal incubation for 20 min at 37 °C. Red corresponded to the normal brain tissues, whilst the infarct tissues were white. After TTC staining, the slices were fixed in 4% paraformaldehyde overnight, the brain slices were then photographed and the infarct area was calculated using Image-Pro Plus 6.0 software (Media Cybernetics, Inc., Rockville, MD). Tests were conducted by an observer blinded to the treatment group. To correct infarct volume (*V_i*) for brain edema, the percentage of the infarction volumes (*I*) were obtained using following formula:

$$I = (V_c - V_i) / V_c \times 100\%$$

V_c = volume of intact contralateral (left) hemisphere

V_i = volume of intact regions of the ipsilateral (right) hemisphere (Zhang et al., 2017).

2.6. Statistical analysis of histological and behavioral assessments

Graphpad prism 5.0 software was used to analyze the data, and the data were expressed as mean ± standard error of the mean (SEM). One-way ANOVA and Student's *t*-test was used to test the significance of differences. A value of *P* < 0.05 was considered to have statistical difference.

2.7. Pathological examination of brain tissue

The third slices of the coronal section with cortex region were immediately fixed in 10% formalin solution overnight and then embedded in paraffin. 4-μm thick sections were cut and then stained with hematoxylin and eosin (HE), NeuN, and TUNEL to examine the pathological change of brain tissue by light microscopy (Pang et al., 2021; Pittet & Conzelmann, 2007).

2.8. Biological sample collection

All rats were anesthetized with chloral hydrate (300 mg/kg, *i.p.*). Blood was sampled from abdominal aorta at 2 h after the last

dosing of LTC, and then collected into natrium citricum anticoagulant tubes and centrifuged at 12 000 r/min for 10 min to yield plasma. A 100 μ L aliquot of plasma was mixed with 300 μ L ACN, 10 μ L 19:0 Lyso PC, and 10 μ L *L*-leucine-5,5,5-*d*₃. The resultant mixtures were centrifuged at 12 000 r/min for 10 min, and the supernatants were transferred into vials for the metabolomic study. Moreover, 10 μ L aliquots of each plasma sample were pooled and parallelly prepared with other plasma sample to yield quality control (QC) sample. QC samples were injected after every eight testing samples for method validation.

2.9. Plasma metabolomic analysis

UltiMate 3000 Hyperbaric LC system (Thermo Fisher Scientific, Bremen, Germany) coupled to Q Exactive MS was employed for LC-MS measurements. Chromatographic separations were conducted on two columns with orthogonal separation mechanisms such as a Waters Acquity HSS T3 (2.1 mm \times 100 mm, 1.8 μ m) column and a Waters XBridge BEH Amide (2.1 mm \times 100 mm, 3.5 μ m) column, corresponding to RPLC and HILIC principles, respectively. For RPLC separations, the mobile phase was composed of methanol (A) and 0.2% aqueous FA (B), and delivered in gradient as follows: 0–1 min, 25%–45% A; 1–3.5 min, 45%–75% A; 3.5–6 min, 75%–100% A; 6–15 min, 100% A; 15–15.1 min, 100%–20% A; and 15.1–18 min, 20% A. On the other side, the mobile phase consisted of ACN (A) and 0.2% aqueous FA (B), and gradient elution was programmed as bellow: 0–7 min, 95%–50% A; 7–9 min, 50% A; 9–9.1 min, 50%–95% A; and 9.1–12 min, 95% A. Regardless of the chromatography principle, the flow rate was always maintained at 0.3 mL/min, and 2 μ L aliquots were injected into the column by the auto-sampler. The column temperature was set at 40 $^{\circ}$ C.

ESI source was operated in the both positive and negative polarities for RPLC, aiming to profile the lipids and fatty acids, respectively. Positive mode was deployed to ionize the amino acids eluted from the HILIC column. The parameters were defined as follows: capillary temperature, 320 $^{\circ}$ C; source voltage and spray voltage, 3.5 kV; sheath gas (nitrogen) flow, 30 arb; and aux gas flow, 10 arb. Data were acquired using full mass scan: resolution as 70 000 FWHM; AGC target, 1×10^6 ; maximum IT, 50 ms; scan range, *m/z* 120–1800 for RPLC system and *m/z* 70–1050 for HILIC system. For precisely structural identification, collision-induced dissociation (CID)-based data dependent on MS/MS (ddMS²) (resolution, 17 500 FWHM; AGC target, 1×10^5 ; maximum IT, 100 ms; loop count, 10; isolation window, *m/z* 4.0; NCE/stepped NCE: 10, 30, 55; minimum AGC target 8×10^3) was also employed.

2.10. Metabolomics data processing and statistical analysis

The raw data were processed using the Thermo Xcalibur software, and Waters Progenesis QI Version 2.3 was responsible for the multivariate statistical analysis. After deconvolution, alignment, peak picking, and structural annotation, successively, the intensities for all detected peaks were tagged with *m/z*-retention time pairs (*m/z*-*t_R*) to generate dataset for RPLC-(+), RPLC(-), and HILIC-(+) separately. Multivariate analyses were conducted after that each data was mean centered and Pareto scaled. Afterwards, the processed data were subjected into an EZinfo software package (Waters Progenesis QI) for principal component analysis (PCA) and orthogonal partial least squares discriminant analysis (OPLS-DA).

The established model was validated with *R*² and *Q*² values. Permutation model by the software SIMCA-P (Software Version 11.5, Umetrics, Umea, Sweden) was also utilized as a cross-validation means to assess whether the method is over-fitting or not. If all the values of *R*² and *Q*² in the permitted model were lower than those of the original model and the *Q*² intercept was close to or under zero, the model was considered as valid (Guillermo et al.,

2012). Thereafter, latent biomarkers were selected by ranking with variable importance in projection (VIP) values, and metabolites with VIP ≥ 2.0 were considered to be potential biomarkers. Moreover, the data include two influencing factors: surgery and medication. For two independent factors, two-way ANOVA analysis was used. In the results, we chose the medication group with *P* < 0.05, MCAO + LTC/MCAO > 1.4 or < 0.7 is the standard for screening different substances. The candidate biomarkers were evaluated by receiver operating characteristics (ROC) curve analysis, which was carried out by R3.6.1. Statistically significant metabolic pathways associated with proposed metabolic biomarkers were elucidated through metabolites biological role (MBRole), which performs an overrepresentation (enrichment) analysis of categorical annotations for a set of compounds of interest. The KEGG database was used as the annotation source, the KEGG compound ID's of metabolites were used as input, and significantly enriched (*P* < 0.05) metabolic and signaling pathways were identified.

3. Results

3.1. Histological and behavioral assessments

To investigate the neuroprotective efficacy of LTC treatment, the anti-inflammatory effect of LTC was observed by HE staining (Fig. 1A). As expected, no histopathological abnormalities and inflammatory cells were observed in the sham group. While in the MCAO group, interstitial edema, atrophy, and pyknosis of glial and neuronal cells occurred in the infarcted area, core area, and marginal area of cerebral cortex. These pathological changes were restricted by LTC treatment. In addition, the inflammatory cell infiltration in the infarcted area in the MCAO + LTC group was significantly lower than that in the MCAO group. *NeuN* showed that the number of *NeuN*⁺ in MCAO group was significantly less than that in sham group, and the number of neurons increased after LTC treatment (Fig. 1B). The results of *Tunel* showed that the number of apoptotic cells in MCAO group was significantly more than that in sham group. After LTC treatment, the number of apoptotic cells decreased in MCAO + LTC group (Fig. 1C). The above results show that LTC may be effective in the treatment of MCAO.

In comparison of the MCAO group, LTC significantly reduced the infarct area from 34.83% to 8.18% in LTC group, according to the TTC staining of cerebral slices (Fig. 2A and B). The neurological damage level was evaluated by an observer blind to the protocol using a five-point scale. Fig. 2C and D illustrated the neurological deficit scores on day 2 and day 7 after surgery, respectively. LTC exerted a satisfactory effect to quickly reduce the neurological deficit score within a single day after the operation. Seven days treatment later, the scores were (0.45 \pm 0.23) and (1.70 \pm 0.95), corresponding to LTC group and MCAO group, respectively.

3.2. Metabolite characterization of samples from MCAO and MCAO + LTC

Representative total ion current chromatograms (TIC) of plasma samples which detected by UHPLC-Q Executive MS in RPLC-(+) mode are shown in Fig. S1, and the representative chromatograms in RPLC(-) and HILIC-(+) modes are shown in Fig. S2. Overall, the peak shape of each substance was acceptable and great resolutions were achieved for most peaks.

After the raw data preprocessing, the data include two influencing factors: surgery and medication. According to the screening criteria, different substances were screened in RPLC(-), RPLC(+), and HILIC-(+). The results showed that 432 different substances were screened from RPLC(-) mode, 374 and 199 ones from RPLC(+) and HILIC-(+) modes, respectively. Subsequently, the unsupervised

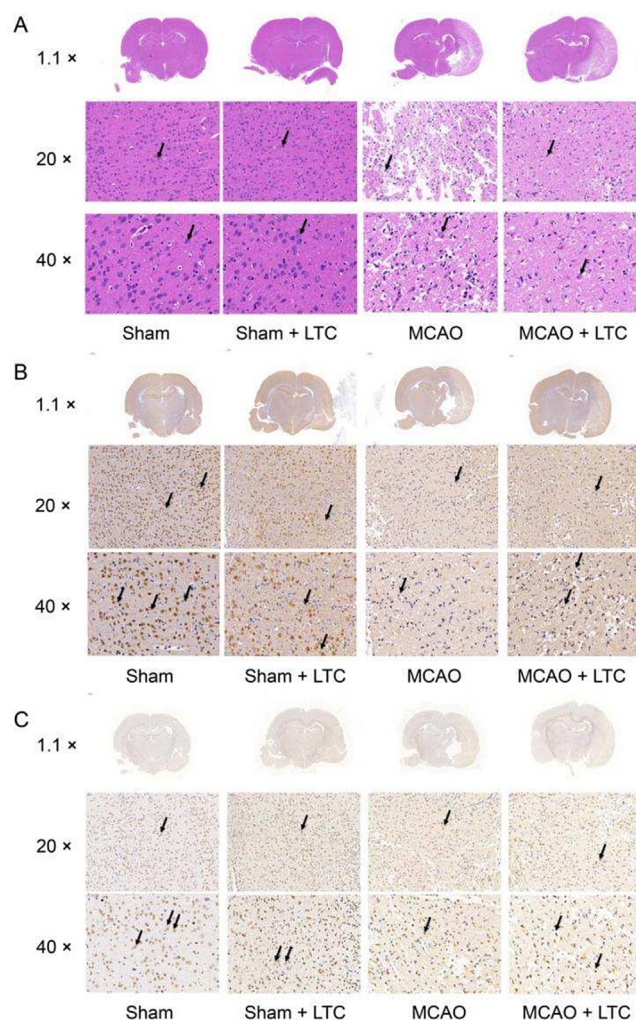


Fig. 1. Pathological abnormalities of brain tissue and neurons restored by LTC, manifested from HE and TUNEL staining and NeuN IHC assay. (A) HE staining, black arrows indicate vacuolation and karyopyknosis of the neuronal cell in the representative photomicrographs; (B) NeuN IHC assay, brown arrows show the positive staining of the neuronal cell in the representative photomicrographs; (C) TUNEL staining, brown arrows indicate apoptotic vascular cells in the representative photomicrographs.

PCA was used to explore the differences among those four groups. Taking the multivariate statistical analysis of the data detected in RPLC-(+) mode as an example, the score plot of PCA (Fig. S3A) showed that the QC samples tightly gathered, suggesting a great system stability within the entire measurement queue. Clear clustering occurred between the MCAO and sham groups with a well goodness of fit ($R^2_X = 0.72$, $Q^2 = 0.43$). The MCAO + LTC group was located between the MCAO and sham groups, suggesting that LTC treatment alleviated the metabolism variations in MCAO model rats. The corresponding plots in RPLC(-) and HILIC (+) modes are illustrated in Fig. S3C and Fig. S3E, respectively.

3.3. Screening biomarkers for LTC treatment

OPLS-DA, that is a supervised pattern recognition technique and advantageous at class discrimination over PCA, was employed to find the different metabolites between each pair of groups. OPLS-DA was modeled for the classification between the MCAO and sham groups as well as between the MCAO + LTC and MCAO groups, respectively. Obviously, significant separation occurred between the MCAO and sham groups, and the MCAO + LTC and MCAO

groups, suggested that great metabolic disorders in plasma were induced by cerebral ischemic reperfusion injury, and after LTC treatment, some endogenous metabolites were restored to the normal levels. Fig. S3B, S3D and S3F show the scores plot from OPLS-DA model for MCAO and MCAO + LTC groups. The parameters of this model ($R^2_Y = 0.96$, $Q^2 = 0.41$) as well as permutation test results could meet the acceptable requirements. Using the VIP, P , and MCAO + LTC/MCAO screening criteria as aforementioned, 118 significant metabolites were screened out and structurally annotated. The corresponding plots in RPLC(-) ion mode and HILIC (+) ion mode are illustrated in Fig. S2. Initially, 79 variables under RPLC(-) ion mode and 55 variables under HILIC (+) ion mode were selected based on the combinations of VIP values.

To reduce errors in the two-factor condition of surgery and LTC, two-factor analysis of variance was carried out. Combination of two-factor analysis of variance and OPLS-DA model, 13 identical metabolites were obtained (Table 1). According to the ROC value of youden index in the table, we found 11 identical metabolites with the Youden index (J) greater than 0.7.

3.4. Correlation and metabolite pathway analysis

As shown in Fig. 3A, using Pearson correlation coefficients, we performed a correlation analysis and found that SM (d16:1/20:1) and SM (d18:1/20:0) correlated well with DG (16:1n7/0:0/18:1n9), DG (20:0/0:0/14:1n5), LysoPC [18:3 (9Z, 12Z, 15Z)], PE (24:1/18:3), and stearyl sphingomyelin were very well correlated. In addition, ganodermic acid TQ and sulfolithocholylglycine, taurohyocholate correlated very well. Trichloroethanol glucuronide correlated well with N_1 -methyl-4-pyridone-3-carboxamide.

The 13 compounds filtered by two-factor analysis and OPLS-DA analysis of MCAO + LTC vs. MCAO groups were also imported into Metaboanalyst 4.0 (<https://www.MetaboAnalyst.ca/>) (Chong, Wishart, & Xia, 2019). As shown in Table 2 and Fig. 3B, the biological roles of these metabolites were determined via metabolic pathway enrichment analyses. LysoPC (20:5), PE (24:1/18:3), and LysoPC [18:3(9Z,12Z,15Z)] belonged to glycerophospholipid metabolism; PE (24:1/18:3) to glycosylphosphatidylinositol (GPI)-anchor biosynthesis; SM (d18:1/20:0), SM (d16:1/20:1), stearyl sphingomyelin to sphingolipid metabolism; and N_1 -methyl-4-pyridone-3-carboxamide to nicotinate and nicotinamide metabolism were disturbed after LTC treatment on MCAO rats.

The network of the remarkable perturbed metabolomic data related to differential lipid species was summarized in Fig. 4 by MetScape analysis (<http://metscape.ncibi.org/index.html>). Results showed mainly the pathways of glycerophospholipid metabolism, GPI-anchor biosynthesis, sphingolipid metabolism and nicotinate and nicotinamide metabolism. Although no relevant pathways were found for DG(16:1n7/0:0/18:1n9), DG(20:0/0:0/14:1n5) and trichloroethanol glucuronide, they may act through glycerophospholipid metabolism and nicotinate and nicotinamide metabolism indicated by correlation analysis.

3.5. Heatmap and ternary analysis

In order to better demonstrate the relationships among the biomarkers and the pathways by which they participate, we classified the metabolites using the HMDB and Lipidmaps databases. As a result, lipids and lipid-like molecules category involved DG (16:1n7/0:0/18:1n9) (diradylglycerols), DG (20:0/0:0/14:1n5) (diradylglycerols), ganodermic acid TQ (triterpenoids), LysoPC (18:3 (9Z,12Z,15Z)) (glycerophosphocholines), LysoPC(20:5) (glycerophosphocholines), PE(24:1/18:3) (glycerophosphocholines), SM(d16:1/20:1) (phosphosphingolipids), SM(d18:1/20:0) (phosphosphingolipids), stearyl sphingomyelin (phosphosphingolipid),

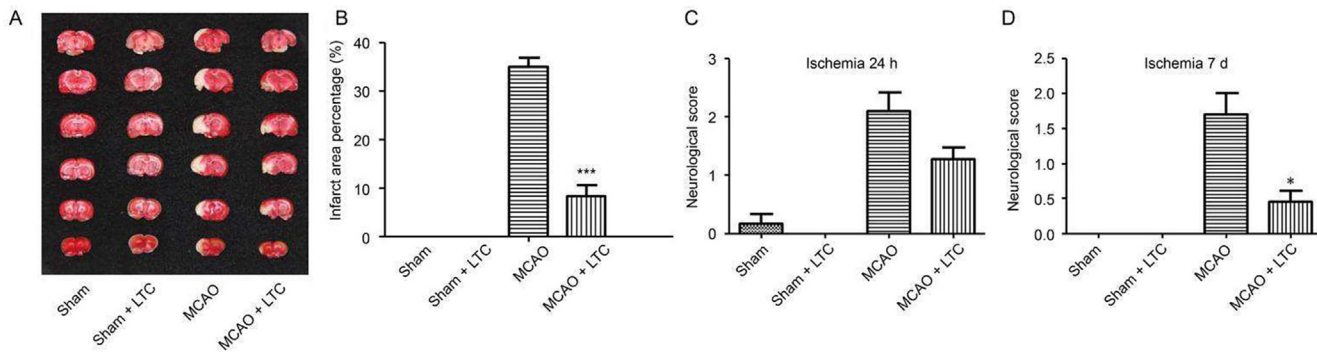


Fig. 2. Infarct regions and neurobehavioral disability restored by LTC treatment, revealed by TTC (2,3,5-triphenyltetrazoliumchloride) staining and neurological scores (mean ± SEM, n = 6). TTC staining of brain (A), infarct area (B), neurological deficit score measurement on 24 h after MCAO (C), neurological deficit score measurement on day 7 after MCAO (D). *P < 0.05, ***P < 0.001, relative to MCAO group.

Sulfolithocholyglycine (bile acids, alcohols and derivatives) and taurohyocholate (bile acids, alcohols and derivatives). Organooxygen compounds category involves N₁-methyl-4-pyridone-3-carboxamide (pyridines and derivatives) and trichloroethanol glucuronide (Fig. 5A), which belongs to sugar acids and derivatives (Fig. 5B).

Heat map analysis using euclidean distance clustering showed that the compounds could separate the MCAO and MCAO-LTC groups well, indicating that the differential molecules as biomarkers were found. Compound clustering showed that lysoPC lipids were closer to trichloroethanol glucuronide, though both belong to phosphosphingolipids (pink color), SM lipids were closer to searoyl sphingomyelin and PE(24:1/18:3). While DG (20:0/0:0/14:1n5) was close to N₁-methyl-4-pyridone-3-carboxamide, DG (16:1n7/0:0/18:1n9) was closer to LysoPC and trichloroethanol glucuronide (Fig. 5A). In addition, we performed a ternary graph analysis of the broad categories to which the compounds belonged. The results showed that the intake of LTC changed the samples from a uniform distribution of sugar-water compounds and lipid molecules to a concentration in the sugar-water compound region (Fig. 5B).

4. Discussion

It has been reported recently that LTC and its component exhibited a protective effect against cerebral ischemia injury (Pan et al., 2021; Xin et al., 2013). Further investigation to the pathology mechanism, our findings indicated that LTC improved interstitial edema, atrophy, and pyknosis of glial and neuronal cells by HE staining, Tunel staining, and NeuN IHC assay method. In addition, LTC exhibited satisfactory effect to quickly reduce the neurological deficit score using TTC staining method. These data proved that LTC had protected against cerebral ischemic-reperfusion injury induced by MCAO/reperfusion.

The neuroprotective effects of LTC on ischemic stroke and the affected metabolic pathways and networks were investigated for the first time using a UPLC-MS-based metabolomics approach combined with multivariate statistical analysis methods. The metabolomics results revealed that 13 biomarkers such as LysoPC, SM, and PE (24:1/18:3) were significantly perturbed in MCAO rats, and 11 of them were restored after LTC treatment. These biomarkers were highly correlated with regulating glycerophospholipid and sphingolipid metabolism, together with bicotinate and nicotinamide metabolism.

Phosphoglycerides are formed by glycerol as the basic skeleton. They are substituted by different groups at C₁-O-position to form polar head clusters, and aliphatic acyl chains at C₂-O- and C₃-O-

sites to form hydrophobic tails. The C₁-O-linked groups govern the glycerophospholipid types, including PA, PS, PE, PC, PI, PG, Cardiolipin, and other subtypes (van Deenen, & de Haas, 1964). PC, also known as lecithin, is an important phosphatidylcholine component in cell membranes. It has been reported that phosphatidylcholine maintains a balance between hydrolysis and biosynthesis: phosphatidylcholine A2, phosphatidylcholine specific hydrolase C and phosphatidylcholine D hydrolyze phosphatidylcholine, while phosphatidylcholine cytidine transferase is the rate-limiting enzyme for the synthesis of phosphatidylcholine (Adibhatla et al., 2006). After acute cerebral ischemia in rats, the activity of these three enzymes increased, resulting in the hydrolysis of phosphatidylcholine and the decrease of the activity of phosphatidylcholine cytidine transfers, which further led to apoptosis (Farooqui, Horrocks, & Farooqui, 2007; Fuchs, Schiller, & Cross, 2007). In this experiment, compared with sham group, the contents of many PCs and PEs were decreased in MCAO group, indicating that PCs and PEs were hydrolyzed, leading to a large number of cell death. Therefore, PCs and PEs could be used as biomarkers related to ischemic stroke. A large number of fatty acids were produced after glycerophospholipids hydrolyzed, and the levels of stearic acid, eicosapentaenoic acid, and other fatty acids in the plasma of rats in the model group were significantly higher than those in the sham-operated group. It has been reported that the stroke patients have a high content of fatty acids in plasma, and fatty acids could be used for early prediction of stroke (Choi et al., 2014). Excessive fatty acids can promote the interaction between leukocytes and endothelial cells, damage the oxidative function of endothelium and mitochondria, promote vascular endothelial inflammatory response, and then participate in the occurrence of cerebrovascular diseases (Bardini, Rotella, & Giannini, 2012). Fatty acids could form to acetyl CoA after β-oxidation *in vivo*, and acetyl CoA is not only the center of the tricarboxylic acid (TCA) cycle, but also involved in butyric acid metabolism and ketone synthesis.

GPI anchoring modification of glycosylphosphatidylinositol is one of the most common post-translational modifications of eukaryotic cell membrane proteins (Kinoshita, Fujita, & Maeda, 2008; Orlean & Menon, 2007; Pittet & Conzelmann, 2007). GPI is responsible for anchoring proteins on the outside of the plasma membrane (Kinoshita, Fujita, & Maeda, 2008). More than 150 proteins in the human body are anchored by GPI (UniProt, 2015). Due to the modification of GPI, GPI-anchored proteins in mammalian cells have unique characteristics, which can bind to the microstructure of cell membrane or partially rich in cholesterol and gangliosides to form homopolymers instantly, and can also indicate release from the cell membrane by cutting part of the GPI. GPI-anchored proteins play an important role in signal transduc-

Table 1
Screening of differential metabolites from MCAO and MACO + LTC.

No.	t _R (min)	Description	m/z	Surgery_P ^a	Medication ^b (P < 0.05)	Surgery - Medication	VIP	Fold change ^c	Youden index
1	1.52	N ₁ -Methyl-4-pyridone-3-carboxamide	153.0657 ([M+H] ⁺)	0.994	0.005	0.525	2.4	1.6	0.778
2	1.59	Stearoyl sphingomyelin	731.6049 ([M+H] ⁺)	0.138	0.018	0.124	4.2	0.5	0.833
3	6.03	Trichloroethanol glucuronide	346.9459 ([M+H] ⁺)	0.112	0.005	0.233	4.8	2	0.63
4	8.03	Sulfolithocholylglycine	512.2685 ([M-H] ⁻)	0.28	0.024	0.278	8.2	0.3	0.759
5	8.91	Ganodermic acid TQ	533.3257 ([M+H] ⁺)	0.055	0.027	0.051	2.6	0.2	0.685
6	8.97	Taurhydrocholate	514.2841 ([M-H] ⁻)	0.094	0.041	0.076	16.5	0.2	0.759
7	9.28	LysoPC(20:5)	542.3240 ([M+H] ⁺)	0.645	0.012	0.24	3.6	1.6	0.944
8	9.30	LysoPC [18:3(9Z,12Z,15Z)]	518.3242 ([M+H] ⁺)	0.645	0.012	0.24	3.6	1.6	0.722
9	12.37	SM(d16:1/20:1)	729.5899 ([M+H] ⁺)	0.106	0.004	0.081	3.3	0.6	0.778
10	13.87	PE(24:1/18:3)	824.6154 ([M+H] ⁺)	0.112	0.025	0.545	2.3	1.4	0.778
11	14.08	SM(d18:1/20:0)	759.6371 ([M+H] ⁺)	0.113	0.01	0.111	3	0.5	0.759
12	14.49	DG(16:1n7/0:0/18:1n9)	615.4956 ([M+H] ⁺)	0.756	0.033	0.488	3.4	1.6	0.704
13	15.47	DG(20:0/0:0/14:1n5)	617.5112 ([M+H] ⁺)	0.405	0.02	0.608	2	1.6	0.778

Note: ^a Surgery: (sham) + (sham + LTC) vs (MCAO + LTC) + (MCAO + LTC); ^b Medication: (sham) + (MCAO) vs (sham + LTC) + (MCAO + LTC); ^c MCAO + LTC vs MCAO.

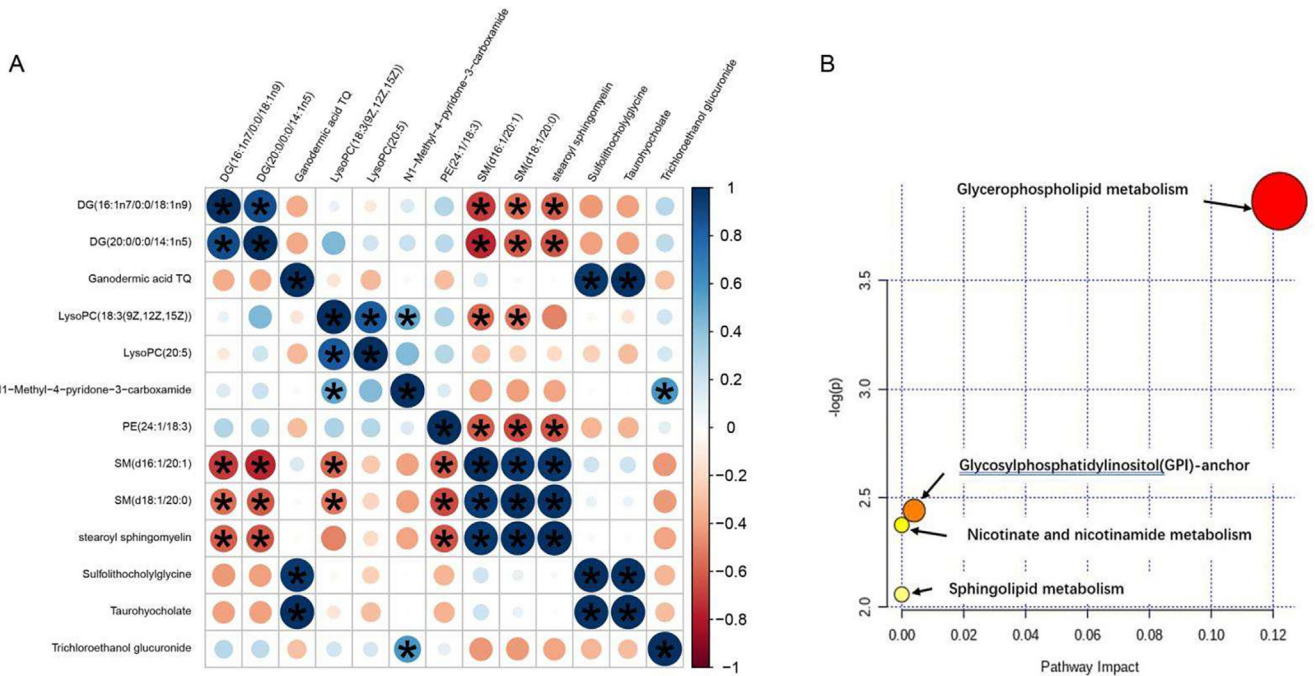


Fig. 3. Correlation and metabolite pathway analysis. (A) The correlation analysis among 13 lipid metabolites. (B) Ingenuity pathway analysis based on the 13 lipid metabolites. The P value (y-axis) was represented by the color of the circle and the pathway impact (x-axis) was indicated by the size of the circle. The involved pathways of the circles are indicated.

tion, cell growth, immune response, cell development and other life processes (Brown, & Rose, 1992; Fujihara et al., 2013; Kondoh et al., 2005; Park et al., 2013; Suzuki et al., 2012).

Nicotinamide is the amide form of nicotinic acid and plays an important role in maintaining normal life activities of cells. It has anti-inflammatory, anti-oxidative and other pharmacological activities, and could also participate in energy metabolism and cell apoptosis inhibition (Park et al., 2013). Nicotinamide can produce NAD⁺, and it has been reported that the level of NAD⁺ in the ipsilateral and contralateral cerebral cortex of MCAO rats decreased after 6 h of successful modeling. Neuronal damage or apoptosis may happen when NAD⁺ was insufficient (Iwahara et al., 2009).

Sphingomyelin signal pathway refers to the conversion of sphingomyelin metabolites such as sphingomyelin (sphingomyelin, SM), neuramide (ceramide, Cer), sphingosine (sphingosine, Sph)

Table 2
Main metabolic pathways of biomarkers based on KEGG.

Pathway names	P value	FDR p	Hits real names
Glycerophospholipid metabolism	0.0003	0.0008	LysoPC(20:5)/PE(24:1/18:3)LysoPC(18:3(9Z,12Z,15Z))
Glycosylphosphatidylinositol (GPI)-anchor biosynthesis	0.0008	0.0013	PE(24:1/18:3)
Sphingolipid metabolism	0.0022	0.0088	SM(d18:1/20:0)SM(d16:1/20:1)
Nicotinate and nicotinamide metabolism	0.0104	0.0313	stearoyl sphingomyelin N ₁ -methyl-4-pyridone-3-carboxamide

FDR p: FDR correction was applied to obtain FDR-corrected P values (q values).

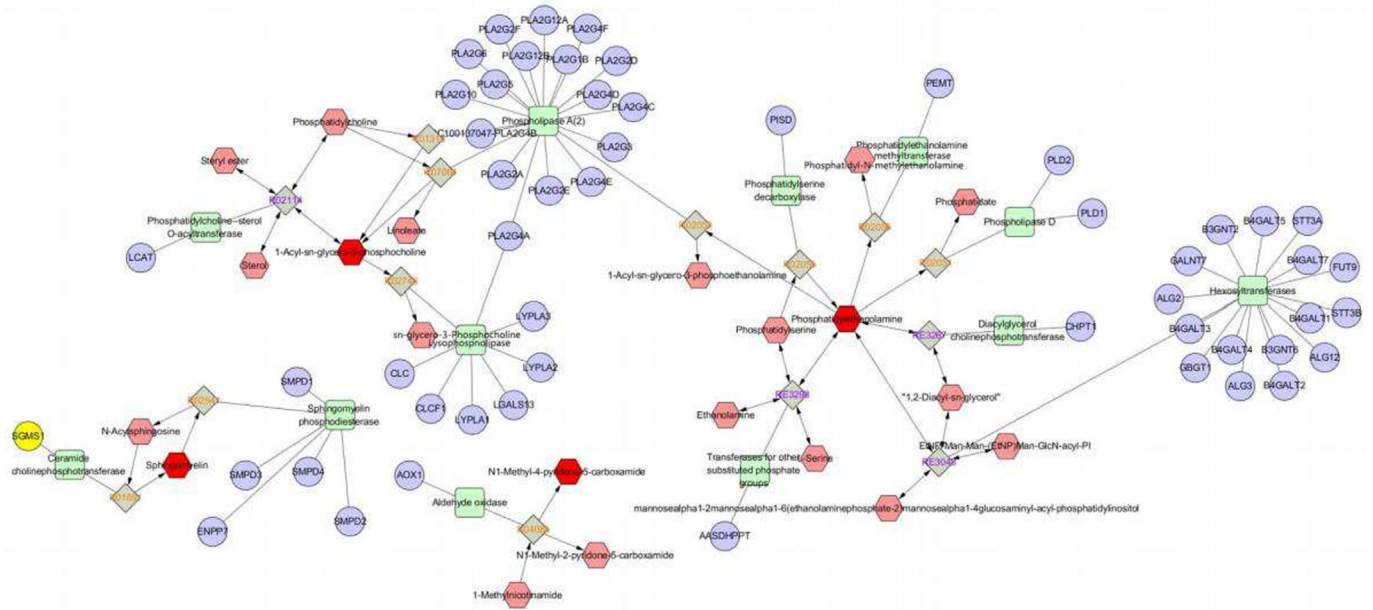


Fig. 4. Network of remarkably perturbed metabolic pathways by MetScape analysis. The red hexagons represent different lipid metabolites identified in our study. Pink is an unidentified metabolite in our study. The purple circle represents related genes. Green squares represent the enzymes participating in the reaction.

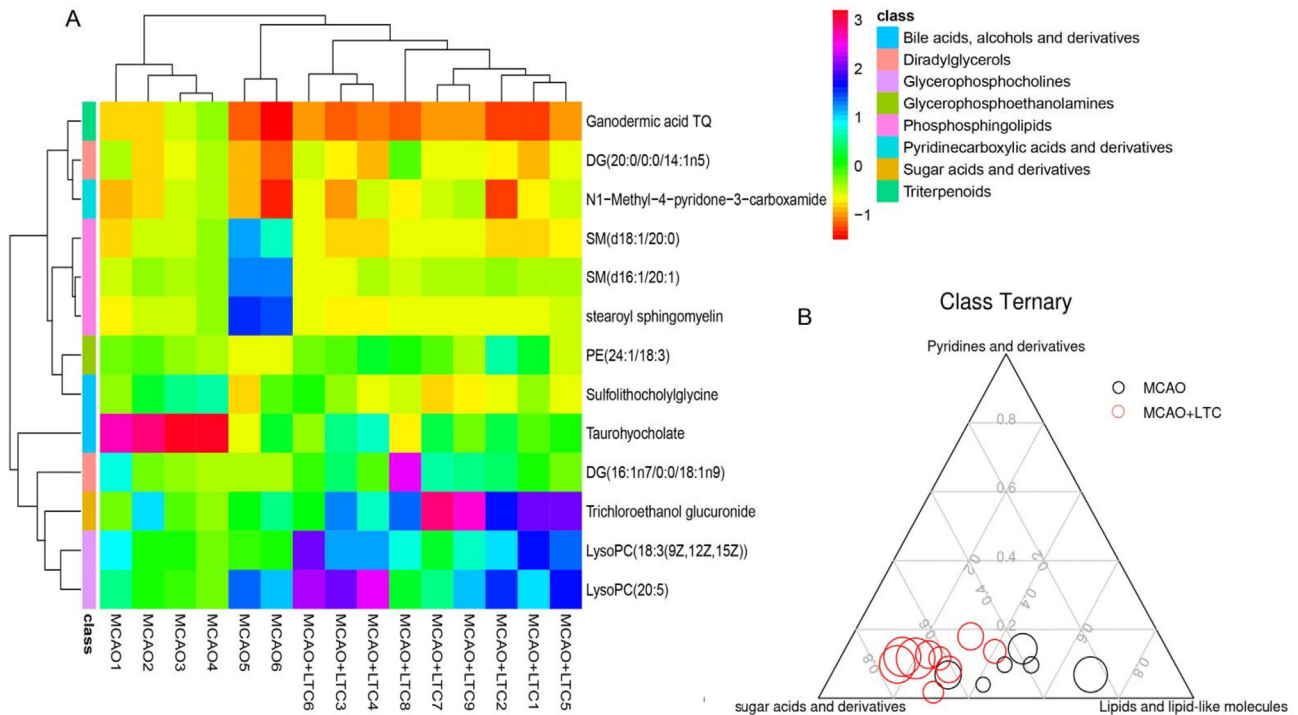


Fig. 5. Heatmap and ternary analysis. (A) Significant changes in serum metabolites are expressed between MCAO and MCAO-LTC groups. The color block represents different categories classified by HMDB or Lipidmaps databases. (B) Ternary plot by 13 metabolites belonged to three categories. Every dot presents one sample from MCAO or MCAO-LTC. Dot size indicates the raw intensity of each metabolites.

and sphingosine 1-phosphate (sphingosine-1-phosphate, S1P) under the action of sphingomyelinase, sphingomyelin synthase (sphingomyelin synthase, SMS), ceramide synthase, sphingosine kinase, phosphorylase and so on. A series of enzymatic pathways in which extracellular signal molecules are introduced into cells through the cell membrane to regulate cell growth, proliferation, apoptosis and differentiation (Yi, Zeng, & He, 2010). SM is an important starting substrate of sphingomyelin signaling pathway, which can be hydrolyzed into Cer; Cer under the action of sphin-

gomyelinase and SM, under the action of SMS, or metabolized into Sph and free fatty acids by ceramidase hydrolysis, and can also be metabolized into brain glycosides, glycosphingolipids and neuramide-1-phosphate by other pathways. Sph is phosphorylated to S1P under the action of sphingosine kinase, and S1P can also be inversely converted to Sph and Cer under certain conditions. SM, Cer, and S1P are important molecules of sphingomyelin signaling pathways. They are continually synthesized and decomposed by enzymes to form a dynamic balance, so as to regulate the physio-

logical and biochemical reactions of the body and maintain the normal physiological function of the body. In recent years, more and more evidence shows that the sphingomyelin signaling pathway is involved in the occurrence and development of heart failure, hypertension, diabetes, fatty liver, Alzheimer's disease and other diseases, and its role in the pathophysiology of has attracted much attention. PE (24:1/18:3) (nervonic acid, NA) is a long chain of monounsaturated omega-9 fatty acids that are particularly abundant in the white matter of the brain. Nervonic acid (C24:1) is an essential molecule for the growth and maintenance of brain and peripheral nervous tissue (Pickens et al., 2015). It is rich in sphingomyelin and is associated with psychiatric disorders. Combined with the results of this study, the efficacy of LTC towards MACO could attribute to that NA may affect the formation of myelin sheath, repair the damaged myelin sheath, and thus play a role.

In the current study, three metabolic pathways were deemed as the main metabolic pathways after ischemic stroke. Among them, glycerophospholipid metabolic were the common metabolic pathways, suggested that the disturbance of some metabolites in these metabolism pathways by MCAO may be restored to a normal state after LTC treatment (Fig. 4).

Studies have shown that the metabolism of flavonoids can not only cause the changes of carbohydrates such as sugar acids, but also affect the changes of bile acids (Fischer et al., 2018; Ma et al., 2020). It has been clarified that the main components of LTC were flavonoids (Pang et al., 2016; Pang et al., 2018; Pang et al., 2021; Su et al., 2014a, 2014b; Sun et al., 2017; Sun et al., 2018; Sun et al., 2019), as well as the type of plasma metabolites transfer towards carbohydrates after intake of LTC as shown in the ternary graph, these results supported our preliminary research work that glucuronidation and sulfonation were major biotransformation pathways of LTC *in vivo* (Sun et al., 2021). The above results indicated that the mechanism of LTC against ischemic stroke may be related to regulating the balance of carbohydrates and lipids, and then affecting downstream pathways, including phospholipid metabolism and bile acid metabolism.

5. Conclusion

In summary, a UHPLC-Q Exactive MS-based metabolomics study was conducted to evaluate the metabolic pathways perturbed by MCAO and to explore the protective mechanism of LTC on cerebral ischemia. It was found that LTC could decrease the behavioral score of rats and reduce the area of cerebral infarction as well. In addition, LTC could restore the metabolic disorders to normal status by regulating the metabolic pathways involving glycerophospholipid metabolism, glycosylphosphatidylinositol (GPI)-anchor biosynthesis, nicotinate and nicotinamide metabolism and sphingolipid metabolism. Moreover, the present study could provide evidences that metabolomics, as systematic approach, revealed its capacity to evaluate the holistic efficacy of TCM, and investigate the molecular mechanism underlying the clinical treatment of LTC on ischemic stroke.

Authors' contributions

Jing Sun: Conceptualization, Methodology, Writing – original draft, Writing – review & editing. **Xianyang Chen:** Formal analysis, Data curation, Writing – review & editing, Methodology, Investigation. **Yongru Wang:** . **Yuelin Song:** Formal analysis, Data curation. **Bo Pan:** Methodology, Investigation. **Bei Fan:** Writing – review & editing, Resources, Visualization. **Fengzhong Wang:** Writing – review & editing, Resources, Visualization. **Xiaonan Chen:** Methodology, Investigation. **Pengfei Tu:** Data curation, Visualization, Supervision. **Jiarui Han:** Formal analysis, Data curation. **Huixia**

Huo: Writing – review & editing, Supervision. **Jun Li:** Supervision, Project administration, Funding acquisition.

Declaration of Competing Interest

The authors declare that they have no known competing financial interests or personal relationships that could have appeared to influence the work reported in this paper.

Acknowledgements

This work was financially supported by the National Natural Science Foundation of China (81573572, 81530097, 32101957), the National Key R&D Program of China (2022YFC2010104), Agricultural Science and Technology Innovation Program of Institute of Food Science and Technology, Chinese Academy of Agricultural Sciences (CAAS-ASTIP-Q2022-IFST-08).

Appendix A. Supplementary data

Supplementary data to this article can be found online at <https://doi.org/10.1016/j.chmed.2022.12.010>.

References

- Aadibhatla, R. M., Hatcher, J. F., Larsen, E. C., Chen, X., Sun, D., & Tsao, F. H. (2006). CDP-choline significantly restores phosphatidylcholine levels by differentially affecting phospholipase A2 and CTP: Phosphocholine cytidyltransferase after stroke. *Journal of Biological Chemistry*, 281(10), 6718–6725.
- Bardini, G., Rotella, C. M., & Giannini, S. (2012). Dyslipidemia and diabetes: Reciprocal impact of impaired lipid metabolism and beta-cell dysfunction on micro- and macrovascular complications. *The Review of Diabetic Studies*, 9(2–3), 82–93.
- Brown, D. A., & Rose, J. K. (1992). Sorting of GPI-anchored proteins to glycolipid-enriched membrane subdomains during transport to the apical cell surface. *Cell*, 68(3), 533–544.
- Choi, J. Y., Kim, J. S., Kim, J. H., Oh, K., Koh, S. B., & Seo, W. K. (2014). High free fatty acid level is associated with recurrent stroke in cardioembolic stroke patients. *Neurology*, 82(13), 1142–1148.
- Chong, J., Wishart, D. S., & Xia, J. (2019). Using MetaboAnalyst 4.0 for comprehensive and integrative metabolomics data analysis. *Current Protocols in Bioinformatics*, 68(1), e86.
- Farooqui, A. A., Horrocks, L. A., & Farooqui, T. (2007). Interactions between neural membrane glycerophospholipid and sphingolipid mediators: A recipe for neural cell survival or suicide. *Journal of Neuroscience Research*, 85(9), 1834–1850.
- Fischer, N., Seo, E. J., & Efferth, T. (2018). Prevention from radiation damage by natural products. *Phytomedicine*, 47, 192–200.
- Fuchs, B., Schiller, J., & Cross, M. A. (2007). Apoptosis-associated changes in the glycerophospholipid composition of hematopoietic progenitor cells monitored by 31P NMR spectroscopy and MALDI-TOF mass spectrometry. *Chemistry and Physics of Lipids*, 150(2), 229–238.
- Fujihara, Y., Tokuhiko, K., Muro, Y., Kondoh, G., Araki, Y., Ikawa, M., & Okabe, M. (2013). Expression of TEX101, regulated by ACE, is essential for the production of fertile mouse spermatozoa. *Proceedings of the National Academy of Sciences of the United States of America*, 110(20), 8111–8116.
- Guillermo, Q., Nuria, P., Juan, C. G., José, V. C., Alberto, F., & Agustín, L. (2012). Chemometric approaches to improve PLS-DA model outcome for predicting human non-alcoholic fatty liver disease using UPLC-MS as a metabolic profiling tool. *Metabolomics*, 8, 86–98.
- Irie, M., Fujimura, Y., Yamato, M., Miura, D., & Wariishi, H. (2014). Integrated MALDI-MS imaging and LC-MS techniques for visualizing spatiotemporal metabolic dynamics in a rat stroke model. *Metabolomics*, 10(3), 473–483.
- Iwahara, N., Hisahara, S., Hayashi, T., & Horio, Y. (2009). Transcriptional activation of NAD⁺-dependent protein deacetylase SIRT1 by nuclear receptor TLX. *Biochemical and Biophysical Research Communications*, 386(4), 671–675.
- Kinoshita, T., Fujita, M., & Maeda, Y. (2008). Biosynthesis, remodeling and functions of mammalian GPI-anchored proteins: Recent progress. *Journal of Biochemistry*, 144(3), 287–294.
- Kondoh, G., Tojo, H., Nakatani, Y., Komazawa, N., Murata, C., Yamagata, K., ... Takeda, J. (2005). Angiotensin-converting enzyme is a GPI-anchored protein releasing factor crucial for fertilization. *Nature Medicine*, 11(2), 160–166.
- Lee, Y., Khan, A., Hong, S., Jee, S. H., & Park, Y. H. (2017). A metabolomic study on high-risk stroke patients determines low levels of serum lysine metabolites: A retrospective cohort study. *Molecular Biosystems*, 13(6), 1109–1120.
- Longa, E. Z., Weinstein, P. R., Carlson, S., & Cummins, R. (1989). Reversible middle cerebral artery occlusion without craniectomy in rats. *Stroke*, 20(1), 84–91.
- Luo, L., Zhen, L., Xu, Y., Yang, Y., Feng, S., Wang, S., & Liang, S. (2016). ¹H NMR-based metabolomics revealed protective effect of Naodesheng bioactive extract on ischemic stroke rats. *Journal of Ethnopharmacology*, 186, 257–269.

- Ma, X., Jiang, Y., Zhang, W., Wang, J., Wang, R., Wang, L., ... Zhao, Y. (2020). Natural products for the prevention and treatment of cholestasis: A review. *Phytotherapy Research*, 34(6), 1291–1309.
- Orlean, P., & Menon, A. K. (2007). Thematic review series: Lipid posttranslational modifications. GPI anchoring of protein in yeast and mammalian cells, or: How we learned to stop worrying and love glycosphospholipids. *Journal of Lipid Research*, 48(5), 993–1011.
- Pan, B., Sun, J., Liu, Z. Y., Wang, L. X., Huo, H. X., Zhao, Y. F., ... Li, J. (2021). Longxuetongluo Capsule protects against cerebral ischemia/reperfusion injury through endoplasmic reticulum stress and MAPK-mediated mechanisms. *Journal of Advanced Research*, 33, 215–225.
- Pang, D. R., Pan, B., Sun, J., Sun, H., Yao, H. N., Song, Y. L., ... Li, J. (2018). Homoisoflavonoid derivatives from the red resin of *Dracaena cochinchinensis*. *Fitoterapia*, 131, 105–111.
- Pang, D. R., Su, X. Q., Zhu, Z. X., Sun, J., Li, Y. T., Song, Y. L., ... Li, J. (2016). Flavonoid dimers from the total phenolic extract of Chinese dragon's blood, the red resin of *Dracaena cochinchinensis*. *Fitoterapia*, 115, 135–141.
- Pang, D. R., Zou, Q. Y., Zhu, Z. X., Wang, X. Y., Pei, Y. J., Huo, H. X., ... Li, J. (2021). Trimeric chalconoids from the total phenolic extract of Chinese dragon's blood (the red resin of *Dracaena cochinchinensis*). *Fitoterapia*, 154, 105029.
- Park, S., Lee, C., Sabharwal, P., Zhang, M., Meyers, C. L., & Sockanathan, S. (2013). GDE2 promotes neurogenesis by glycosylphosphatidylinositol-anchor cleavage of RECK. *Science*, 339(6117), 324–328.
- Pickens, C. A., Sordillo, L. M., Comstock, S. S., Harris, W. S., Hortos, K., Kovan, B., & Fenton, J. I. (2015). Plasma phospholipids, non-esterified plasma polyunsaturated fatty acids and oxylipids are associated with BMI. *Prostaglandins Leukotrienes and Essential Fatty Acids*, 95, 31–40.
- Pittet, M., & Conzelmann, A. (2007). Biosynthesis and function of GPI proteins in the yeast *Saccharomyces cerevisiae*. *Biochimica et Biophysica Acta*, 1771(3), 405–420.
- Qin, J. P., Lin, X., Pan, Y. Z., Li, J. C., Sun, Y. C., Huang, W. Z., Wang, Z. Z., & Xiao, W. (2015). Quality assessment of Longxue Tongluo Capsule based on HPLC fingerprint and multi-components simultaneous determination. *Chinese Traditional and Herbal Drugs*, 46(20), 3028–3033.
- Su, X. Q., Li, M. M., Gu, Y. F., Sun, J., Zhang, J., Huang, Z., ... Tu, P. F. (2014a). Phenolic constituents from *Draconis Resina*. *Chinese Traditional and Herbal Drugs*, 45(11), 1511–1514.
- Su, X. Q., Song, Y. L., Zhang, J., Huo, H. X., Huang, Z., Zheng, J., ... Tu, P. F. (2014b). Dihydrochalcones and homoisoflavanes from the red resin of *Dracaena cochinchinensis* (Chinese dragon's blood). *Fitoterapia*, 99, 64–71.
- Sun, J., Huo, H. X., Song, Y. L., Zheng, J., Zhao, Y. F., Huang, W. Z., ... Li, J. (2018). Method development and application for multi-component quantification in rats after oral administration of Longxuetongluo Capsule by UHPLC-MS/MS. *Journal of Pharmaceutical and Biomedical Analysis*, 156, 252–262.
- Sun, J., Liu, J. N., Fan, B., Chen, X. N., Pang, D. R., Zheng, J., ... Li, J. (2019). Phenolic constituents, pharmacological activities, quality control, and metabolism of *Dracaena* species: A review. *Journal of Ethnopharmacology*, 244, 112138.
- Sun, J., Liu, J. N., Li, Y. T., Huo, H. X., Xu, X., Xia, H., ... Li, J. (2021). Study on metabolites of Longxue Tongluo Capsule *in vivo* by LC-IT-TOF-MS. *China Journal of Chinese Materia Medica*, 46(18), 4841–4848.
- Sun, J., Song, Y., Sun, H., Liu, W., Zhang, Y., Zheng, J., ... Li, J. (2017). Characterization and quantitative analysis of phenolic derivatives in Longxuetongluo Capsule by HPLC-DAD-IT-TOF-MS. *Journal of Pharmaceutical and Biomedical Analysis*, 145, 462–472.
- Suzuki, K. G., Kasai, R. S., Hirose, K. M., Nemoto, Y. L., Ishibashi, M., Miwa, Y., ... Kusumi, A. (2012). Transient GPI-anchored protein homodimers are units for raft organization and function. *Nature Chemical Biology*, 8(9), 774–783.
- UniProt, C. (2015). UniProt: A hub for protein information. *Nucleic Acids Research*, 43, D204–D212.
- van Deenen, L. L., & de Haas, G. H. (1964). The synthesis of phosphoglycerides and some biochemical applications. *Advances in Lipid Research*, 2, 167–234.
- Xin, N., Yang, F. J., Li, Y., Li, Y. J., Dai, R. J., Meng, W. W., ... Deng, Y. L. (2013). Dragon's blood dropping pills have protective effects on focal cerebral ischemia rats model. *Phytomedicine*, 21(1), 68–74.
- Yi, J. P., Zeng, M., & He, X. X. (2016). The role of sphingomyelin signaling pathway in the pathogenesis of pulmonary fibrosis. *Chinese Journal of Pharmacology and Toxicology*, 30(02), 158–164.
- Zhang, Q., Wang, J., Liao, S., Li, P., Xu, D., Lv, Y., ... Kong, L. (2017). Optimization of Huang-Lian-Jie-Du-Decoction for ischemic stroke treatment and mechanistic study by metabolomic profiling and network analysis. *Frontiers in Pharmacology*, 8, 165.
- Zheng, J., Liu, B. L., Lun, Q. X., Gu, X. P., Pan, B., Zhao, Y. F., ... Tu, P. F. (2016). Longxuetongluo capsule inhibits atherosclerosis progression in high-fat diet-induced *ApoE^{-/-}* mice by improving endothelial dysfunction. *Atherosclerosis*, 255, 156–163.
- Zheng, J., Liu, B. L., Lun, Q. X., Yao, W. J., Zhao, Y. F., Xiao, W., ... Tu, P. F. (2016). Longxuetongluo Capsule improves erythrocyte function against lipid peroxidation and abnormal hemorheological parameters in high fat diet-induced *ApoE^{-/-}* mice. *Oxidative Medicine and Cellular Longevity*, 2016, 2603219.